DIELECTRIC LASER ACCELERATION OF ELECTRONS WITH DOUBLE GRATING STRUCTURE*

Zhaofu Chen†, The University of Tokyo, Tokyo, Japan
Kazuyoshi Koyama, Mitsuru Uesaka,The University of Tokyo, Tokai, Japan
Mitsuhiro Yoshida, High Energy Accelerator Research Organization, Tsukuba, Japan

Abstract

The dielectric laser accelerator (DLAs) has attracted increasing interest in the recent years due to its potential to miniaturize the accelerator. We propose a double grating structure powered by obliquely incident laser for subrelativistic electrons. The structure enables a symmetric accelerating mode which results in lower energy spread.

INTRODUCTION

Dielectric laser accelerator (DLA) with dielectric structure has great potential for the miniaturization of accelerator with its high accelerating gradient enabled by the high damage thresholds of dielectric materials in optical region [1, 2]. Recently, by leveraging the well-developed industrial fabrication capabilities and the commercially available high-power lasers, accelerating gradient of 690 MV/m has been achieved with fused silica dual-grating DLA for relativistic electrons [3, 4], and accelerating gradient of 370 MV/m has been obtained with silicon dual-pillar DLA for nonrelativistic electrons [5, 6].

Here, we present a double grating structure for the acceleration of subrelativistic electrons. The structure is a modification from the double structure experimentally demonstrated by Leedle et al. [6–11], but with a oblique-angle incident laser. The oblique angle enables easier fabrication of the grating and the double grating structure result in a rather uniform accelerating field across the channel.

SINGLE GRATING

To understand the accelerating mode in double grating which is the superposition of modes from each single grating, we start from the evanescent modes at single grating. Figure 1 shows the single grating and the longitudinal electric field of the accelerating mode. The laser is incident from above in the x direction, the electron is propagating along z direction. For simplicity, we constraint our discussion on the case of TM polarization in which the electric field is perpendicular to the groove direction, which is required for the acceleration.

At a single grating with period Λ, the incident plane wave with wavelength λ excites a series of spatial harmonics in its vicinity with field profiles given by:

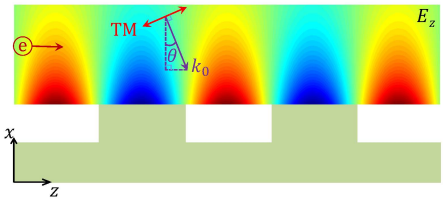

Figure 1: Cross section of the grating discussed in this paper and the longitudinal electric field of the accelerating mode.

$$H_{y,n}(x,z) = H_0 e^{-jk_{x,n}x - jk_{z,n}z} \quad (1)$$

$$E_{x,n}(x,z) = \frac{k_z}{\omega\epsilon} H_y \quad (2)$$

$$E_{z,n}(x,z) = \frac{-k_x}{\omega\epsilon} H_y \quad (3)$$

with θ the incident angle, $n = 0, \pm1, \pm2, \ldots$ the order number, $k_0 = 2\pi/\lambda$ the wave number in free space, the z component of the wave vector $k_{z,n} = k_0 \sin(\theta) + nk_p$ with $k_p = 2\pi/\Lambda$.

In the longitudinal direction, the phase velocity of these harmonics could be written as $v_{ph,n} = \omega/k_{z,n}$. The synchronicity condition between the electron and spatial harmonic with order number s results in

$$k_{z,s} = k_0/\beta_s \quad (4)$$

$$k_{x,s} = ik_0/(\beta_s\gamma_s) \quad (5)$$

where β_s is the electron velocity v_s normalized to the speed of light c. We can describe the synchronicity condition with the ratio of grating period Λ to laser wavelength λ:

$$\frac{\Lambda}{\lambda} = \frac{\beta n}{1 - \beta \sin\theta} \quad (6)$$

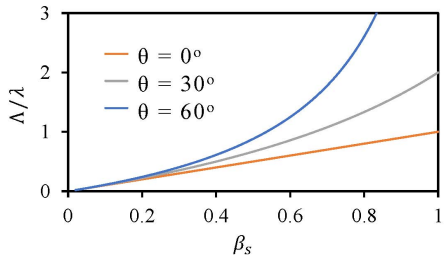

Figure 2: Required grating period Λ vs incident angle θ.

* Work supported by KAKENHI, Grant-in-Aid for Scientific Research (B) 15H03595
† chen.zhaofu@nuclear.jp

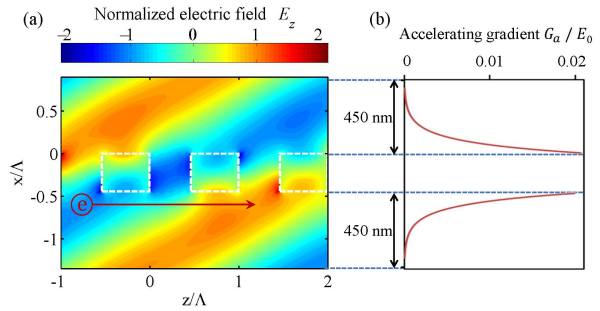

Figure 3: Simulated longitudinal electric field in optimized SiO_2 single grating structure (a) and accelerating gradient around it (b).

In Fig. 2 we show the required grating period as a function of incident angle θ and normalized electron velocity β_s. It is clear that the grating period becomes larger with an oblique incident angle, thus the difficulty in fabrication could be relaxed, which is desirable for electron with low β [12].

With $\Gamma_s = 1/ik_{x,s}$, we can rewritten the field profiles as

$$H_{y,s}(x,z) = H_0 e^{-x/\Gamma_s} e^{-j(k_{z,s}z)} \quad (7)$$

$$E_{x,s}(x,z) = \frac{1}{\beta_s}\sqrt{\frac{\mu_0}{\epsilon_0}} H_0 e^{-x/\Gamma_s} e^{-j(k_{z,s}z)} \quad (8)$$

$$E_{z,s}(x,z) = \frac{-i}{\beta_s\gamma_s}\sqrt{\frac{\mu_0}{\epsilon_0}} H_0 e^{-x/\Gamma_s} e^{-j(k_{z,s}z)} \quad (9)$$

The imaginary value of k_x as shown in Eq. 5 indicates that the accelerating field is evanescent and fall off exponentially with an increasing distance from the grating surface in x direction, as shown in Fig. 3. The skew profile is not desirable for accelerator since it results in large energy spread [13].

DOUBLE GRATING

To produce a symmetric mode, we use the double grating as shown in Fig. 4. The superposition of evanescent modes from each grating forms the accelerating mode inside the channel, thus a more uniform profile could be obtained.

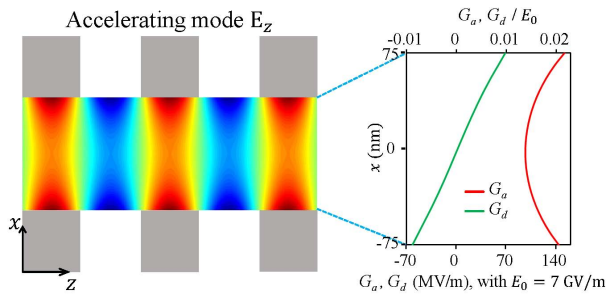

Figure 4: Left: Schematic of the double grating discussed in this paper and the longitudinal electric field of the accelerating mode. Right: Accelerating gradient G_a and deflecting gradient G_d across the channel.

The accelerating mode profiles can be given by

$$H_{y,s}(x) = 2\sqrt{H_u H_d}\sinh\left[\frac{x}{\Gamma_s} + \frac{1}{2}\ln(\frac{H_d}{H_u})\right] \quad (10)$$

$$E_{x,s}(x) = \frac{2\sqrt{H_u H_d}}{\beta_s}\sqrt{\frac{\mu_0}{\epsilon_0}}\sinh\left[\frac{x}{\Gamma_s} + \frac{1}{2}\ln(\frac{H_d}{H_u})\right] \quad (11)$$

$$E_{z,s}(x) = \frac{i2\sqrt{H_u H_d}}{\beta_s\gamma_s}\sqrt{\frac{\mu_0}{\epsilon_0}}\cosh\left[\frac{x}{\Gamma_s} + \frac{1}{2}\ln(\frac{H_d}{H_u})\right] \quad (12)$$

where H_u and H_d are the amplitudes of modes at the channel center from above and below, respectively. Eq. 10, Eq. 11 and Eq. 12 indicate that the axis of the accelerating mode may not be located at the channel center, depending on the amplitude of modes from single grating.

The Lorentz force experienced by the synchronous electron in the channel can be given by

$$\begin{bmatrix}F_x\\F_y\\F_z\end{bmatrix} = \begin{bmatrix}\frac{2\sqrt{H_u H_d}q}{\beta_s\gamma_s^2}\sqrt{\frac{\mu_0}{\epsilon_0}}\sinh\left[\frac{x}{\Gamma_s} + \frac{1}{2}\ln(\frac{H_d}{H_u})\right]e^{i(\omega t - k_{z,s}z - \phi_0)}\\0\\\frac{i2\sqrt{H_u H_d}q}{\beta_s\gamma_s}\sqrt{\frac{\mu_0}{\epsilon_0}}\cosh\left[\frac{x}{\Gamma_s} + \frac{1}{2}\ln(\frac{H_d}{H_u})\right]e^{i(\omega t - k_{z,s}z - \phi_0)}\end{bmatrix} \quad (13)$$

where ϕ_0 is the start phase of electron in the optical cycle.

For the case where $H_d = H_u$, the accelerating electric field in the channel is symmetric, as shown in Fig. 4. With the accelerating gradient at channel center $G_{a,0} = \frac{2H_u q}{\beta_s\gamma_s}\sqrt{\frac{\mu_0}{\epsilon_0}}$, the Lorentz force experienced by the synchronous electron in the channel can be rewritten as Eq. 14. It can be seen that the accelerating mode has a rather uniform electric field profile around the axis, which is desirable for the acceleration of electrons.

$$\begin{bmatrix}F_x\\F_y\\F_z\end{bmatrix} = \begin{bmatrix}-G_{a,0}\sinh(x/\Gamma_s)\cos(\omega t - k_{z,s}z - \phi_0)/\gamma_s\\0\\G_{a,0}\cosh(x/\Gamma_s)\sin(\omega t - k_{z,s}z - \phi_0)\end{bmatrix} \quad (14)$$

ACCELERATION OF ELECTRONS

Here, we focus on the case where the first order spatial harmonic is used for the acceleration. As the electron gains energy, the relative phase of the electron with respect to the accelerating mode changes as the electron gains energy, known as the dephasing process, which may lead to decreasing of acceleration gradient, or even deceleration. In this case, the energy gain depends not only the accelerating ratio between the maximum gradient and the electric field in the grating material G_a/E_0, but also the changing of the relative phase of electron with respect to the optical cycle. To estimate the energy gain, we have to study the effect of dephasing on the acceleration, i.e., how the gradient changes with the distance upon dephasing.

Electrons with kinetic energy of 50 keV are injected into the channel with width d = 150 nm. The grating has a length of 30 μm, including 71 periods. In the simulation, identical accelerating efficiency G_a/E_0 and deflecting efficiency G_d/E_0 in Fig. 4 are used, with $G_{a,0}/E_0 = 0.015$ at channel center. The Gaussian laser pulse with surface-normal

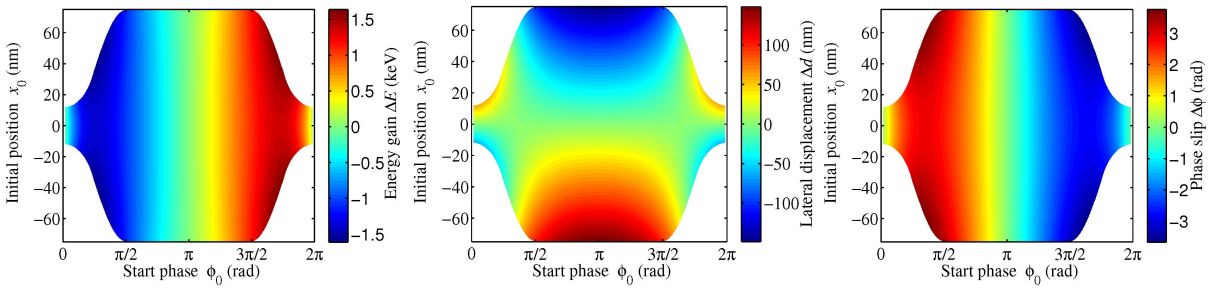

Figure 5: The energy gain ΔE (left), lateral displacement Δd (mid) and phase slippage $\Delta\phi$ (right) of electron as a function of start phase ϕ_0 and initial distance d_0 from the grating below. The white area represents those electrons which are deflected and crash into the dielectric grating.

incidence has an average electric field

$$E_0(z,t) = E_p \exp\left[-(\frac{z - w_1/2}{w_1})^2 - 2\ln(2)(\frac{t - \tau_p/2}{\tau_p})^2\right] \tag{15}$$

where peak field $E_p = 6.7$ GV/m, pulse duration $\tau_p = 100$ fs and waist radius $w_1 = 10$ μm. In the synchronous frame the average electric field experienced by electrons can be written as

$$E_0(z) = E_p \exp\left[-(\frac{z}{w_{int}})^2\right] \tag{16}$$

with

$$w_{int} = \left(\frac{1}{w_1^2} + \frac{2\ln(2)}{(\beta_s c\tau_p)^2}\right)^{-1/2} \tag{17}$$

For clarity, we use subscript s to represent the electrons which are synchronous with the first order spatial harmonic, and subscript e to represent instantaneous parameters for the electrons traversing the grating. Here, we assume $\Delta\beta_e/\beta_e \ll 1$, which is true when the electron's energy gain over one wavelength of the incident field is well below the electron's rest energy m_0c^2, i.e., $G_a \ll m_0c^2/\lambda \approx 496$ GV/m. In a DLA driven by an infrared laser, the general acceleration gradient $G_a < 10$ GV/m, so that the assumption is valid.

Since the electrons' transverse velocity is much smaller than the longitudinal velocity, so we can neglect the contribution of the transverse velocity to the total kinetic energy in the longitudinal motion equation. From the theorem of kinetic energy, we obtain the longitudinal motion equation, where $\phi = \omega t - k_z z - \phi_0$ represents the phase of electron in the optical cycle

$$\frac{\mathrm{d}\gamma_e m_0 c^2}{\mathrm{d}z} = \mathrm{Re}(F_z) \tag{18}$$

$$\frac{\mathrm{d}\phi}{\mathrm{d}z} = k_0\left(\frac{1}{\beta_s} - \frac{\gamma_e}{\sqrt{\gamma_e^2 - 1}}\right) \tag{19}$$

The transverse motion equation can be given by

$$\frac{\mathrm{d}\gamma_e m_0 v_x}{\mathrm{d}t} = \mathrm{Re}(F_x) \tag{20}$$

$$\frac{\mathrm{d}x}{\mathrm{d}t} = v_x \tag{21}$$

By using $\frac{\mathrm{d}}{\mathrm{d}t} = \beta_e c\frac{\mathrm{d}}{\mathrm{d}z}$, equation (20) and (21) can rewritten as

$$\frac{\mathrm{d}\gamma_e m_0 v_x}{\mathrm{d}z} = \frac{1}{\beta_e c}\mathrm{Re}(F_x) \tag{22}$$

$$\frac{\mathrm{d}x}{\mathrm{d}z} = \frac{v_x}{\beta_e c} \tag{23}$$

With Eq. 18, Eq. 19, Eq. 22 and Eq. 23, we could estimate the electron parameters at the end of grating, neglecting the wake field and space charge effect. For one 50 keV electron traveling through the channel, the energy gain, the lateral displacement and the phase slippage vs. the start phase ϕ and x position are shown in Fig. 5. The cosh accelerating field profile leads to a rather uniform energy gain around channel center, which is useful for many applications. It can be also seen that due to the transverse deflection, some electrons will be deflected into the grating. The electron-wave interaction dependence on start phase as shown in Fig. 5 determines that operation with the longitudinal focusing leads to transverse defocusing, which is in agreement with Earnshaw's theorem [14]. To stably accelerate electron, external focusing component is needed.

In Fig. 6 we show the instantaneous parameters of one electron launched at the channel center at an initial phase of $3\pi/2$ as a function of the longitudinal posizion z, including the kinetic energy E_k, the acceleration gradient G_a, the

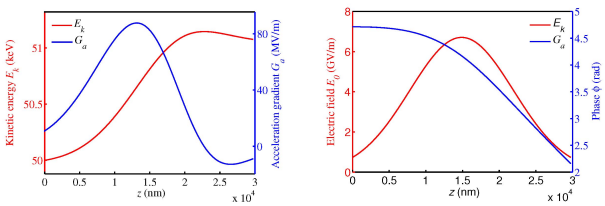

Figure 6: Instantaneous electron parameters as a function of z position. We show the instantaneous kinetic energy E_k (left: red curve), the acceleration gradient G_a (left: blue curve), the average laser electric field experienced by electron E_0 (right: red curve) and the phase of electron in the optical cycle ϕ (right: blue curve). The 50 keV electrons are launched at start phase $\phi = 3\pi/2$ at the channel center $x = 0$ nm .

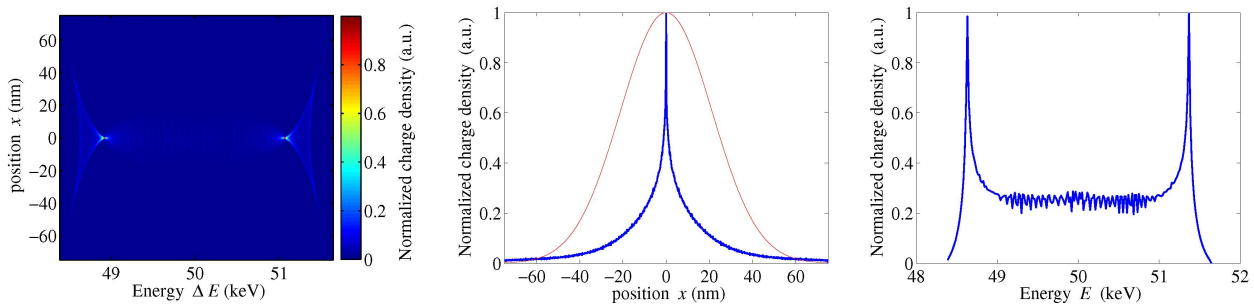

Figure 7: Left: The normalized electron charge density after interaction. Mid: The normalized electron charge density dependence on the position$x$ before (red) and after (blue) interaction. Right: The normalized electron charge density dependence on the energy E. The electron beam density is normalized to 1.

laser electric field amplitude experienced by the electron E_0 and the phase of electron in the optical cycle ϕ. The lateral displacement of the electron is zero due to the vanishing deflection at channel center.It is shown that the dephasing effect could be so severe that the electron is decelerated after initial acceleration, i.e. the electron moves from the acceleration phase to the deceleration phase. By adjusting the grating period according to electron energy variations, the dephasing problem could be alleviated and a higher energy gain could be obtained.

To study the density distribution after interaction, a simplified 2D model is used in the estimation, with the laser and electron beam assumed to be uniform along y direction. For one electron beam traversing the channel, the charge density after interaction are shown in Fig. 7. The temporal envelope and the spatial envelope are taken into account, which are identical with Eq. 15. A Gaussian electron bunch of transverse waist radius w_e = 30nm is launched at the channel center. For simplicity, the density in electron bunch is set to be temporally constant and the pulse duration is one optical cycle. The electron beam energy spread and beam divergence are neglected. It can be seen that the proportion of electron around the channel center becomes higher after interaction, which is the result of sinh deflecting field. There are two distinct charge peaks at channel center, with energy 48.6 keV and 51.4 keV, respectively.

CONCLUSION

We present the study of a double grating structure for the acceleration of 50 keV electrons. By using the obliquely incident laser, the difficulty in fabrication of the grating structure could be alleviated. The uniform accelerating field around the channel center, which is formed by superposition of the evanescent modes from the single grating at each side, is desirable for a variety of applications, such as table-top cancer therapy and university-scale light sources.

ACKNOWLEDGEMENT

We thank R. Zhang, T. Shibuya and T. Natsui for helpful discussions.

REFERENCES

[1] R. J. England *et al.*, “Dielectric laser accelerators”, Rev. Mod. Phys., vol. 86, no. 4, pp. 1337-1389, 2014.

[2] R. J. England, “Review of Laser-Driven Photonic Structure-Based Particle Acceleration,” IEEE J. Sel. Top. QUANTUM Electron., vol. 22, no. 2, 2016.

[3] K. P. Wootton *et al.*, “Demonstration of acceleration of relativistic electrons at a dielectric microstructure using femtosecond laser pulses”, Opt. Lett., vol. 41, no. 12, pp. 2696–2699, Jun. 2016.

[4] E. A. Peralta *et al.*, “Demonstration of electron acceleration in a laser-driven dielectric microstructure”, Nature, 2013.

[5] K. J. Leedle *et al.*, “Laser acceleration and deflection of 96.3 keV electrons with a silicon dielectric structure”, Optica, vol. 2, no. 2, pp. 158–161, 2015.

[6] K. J. Leedle *et al.*, “Dielectric laser acceleration of sub-100 keV electrons with silicon dual-pillar grating structures”, Opt. Lett., vol. 40, no. 18, pp. 4344-4347, 2015.

[7] T. Plettner, R. L. Byer, and B. Montazeri, “Electromagnetic forces in the vacuum region of laser-driven layered grating structures,” J. Mod. Opt., vol. 58, no. 17, pp. 1518–1528, 2011.

[8] K. Koyama *et al.*, “Parameter study of a laser-driven dielectric accelerator for radiobiology research,” J. Phys. B At. Mol. Opt. Phys., vol. 47, no. 23, p. 234005, 2014.

[9] K. Koyama *et al.*, "Laser driven dielectric accelerator in the non-relativistic energy region," in Proc. of IPAC’16, Busan, Korea, paper TUPMY017, p. 1585.

[10] K. Koyama *et al.*, "Development of a laser driven dielectric accelerator for radiobiology research," in Proc. of IPAC’17, Copenhagen, Denmark, paper WEPVA011, p. 3272.

[11] Z. Chen *et al.*, "Numerical study of dielectric laser acceleration of nonrelativistic electrons with colonnade structure," AIP Conf. Proc. vol. 1812, p. 060005, 2017.

[12] S. Otsuki *et al.*, "Development of on-chip radiation source using dielectric laser accelerator," in Proc. of IPAC’14, Dresden, Germany, paper TUPME037, p. 1434.

[13] J. Breuer and P. Hommelhoff, “Laser-Based Acceleration of Nonrelativistic Electrons at a Dielectric Structure,” Phys. Rev. Lett., vol. 111, no. 13, p. 134803, 2013.

[14] S. Earnshaw, “On the nature of the molecular forces which regulate the constitution of the luminiferous ether,” Trans. Camb. Phil. Soc., vol. 7, no. 13, pp. 97-112, 1842.